JACC: ADVANCES VOL. 5, NO. 4, 2026

ORIGINAL RESEARCH

EMERGING TECHNOLOGIES AND INNOVATIONS

Wearable SENsor to Diagnose and Assess SEverity of Aortic Stenosis (SENSE-AS)

A Proof-of-Concept Study

Aniruddh Srinivasan, BS,[a] Lamis El Harake, MD,[b] Edgar D. Torres Fernandez, MD,[c] John Saleeb, BS,[a] Jacob Trueb, MCS,[a] James D. Flaherty, MD,[b,c] Ranya Sweis, MD,[b,c] Sanjiv Shah, MD,[b,c] James D. Thomas, MD,[b,c] Akhil Narang, MD,[b,c] John A. Rogers, PhD,[d,e,f,g] Yayun Du, PhD,[h,i,j,k,l] Paul C. Cremer, MD[b,c]

ABSTRACT

BACKGROUND Aortic stenosis (AS) is a common disease with delays in diagnosis and treatment. Wearable sensors may provide a scalable, noninvasive method to diagnose, assess severity, and monitor AS.

OBJECTIVES The primary objective was to quantify the correlation between Doppler-derived aortic valve (AV) acceleration time (AT) and sensor-derived AT; the secondary objective was to train machine learning models using sensor data to predict maximal transvalvular velocity (Vmax).

METHODS This prospective, single-center case-control study enrolled 40 subjects with severe (n = 10), moderate (n = 10), and mild (n = 10) AS according to echocardiography guidelines, along with controls without AS (n = 10) who were age- and sex-matched to the severe AS cohort. At the time of echocardiography, patients wore a sensor simultaneously recording electrocardiogram, seismocardiogram, and phonocardiogram signals.

RESULTS The mean age across groups was 77.8 years, and 55% were female (n = 22). Sensor-derived AT showed a strong correlation with Doppler AT (r = 0.85; 95% CI: 0.73-0.92; $P < 0.001$). Groupwise comparisons demonstrated progressively longer AT from controls through increasing AS severities ($P < 0.01$). Predictions on unseen patient data from a machine learning model trained on a limited subset of AS patient recordings (n = 32) correlated with AV Vmax (r = 0.76; 95% CI: 0.68-0.83; $P < 0.001$).

CONCLUSIONS A chest-worn multimodal wearable sensor accurately measures AV AT and predicts AV Vmax, supporting the feasibility of accessible, lower-cost tools for early detection and longitudinal monitoring of AS. (JACC Adv. 2026;5:102699) © 2026 The Authors. Published by Elsevier on behalf of the American College of Cardiology Foundation. This is an open access article under the CC BY-NC-ND license (http://creativecommons.org/licenses/by-nc-nd/4.0/).

From the [a]Querry Simpson Institute for Bioelectronics, Northwestern University, Evanston, Illinois, USA; [b]Northwestern University, Feinberg School of Medicine, Chicago, Illinois, USA; [c]Bluhm Cardiovascular Institute, Division of Cardiology, Chicago, Illinois, USA; [d]Department of Material Science and Engineering, Northwestern University, Evanston, Illinois, USA; [e]Department of Biomedical Engineering, Northwestern University, Evanston, Illinois, USA; [f]Department of Mechanical Engineering, Northwestern University, Evanston, Illinois, USA; [g]Department of Neurological Surgery, Feinberg School of Medicine, Northwestern University, Chicago, Illinois, USA; [h]Department of Electrical and Computer Engineering, Vanderbilt University, Nashville, Tennessee, USA; [i]Department of Computer Science, Vanderbilt University, Nashville, Tennessee, USA; [j]Department of Mechanical Engineering, Vanderbilt University, Nashville, Tennessee, USA; [k]Department of Biomedical Engineering, Vanderbilt University, Nashville, Tennessee, USA; and the [l]Vanderbilt Institute for Surgery and Engineering, Vanderbilt University, Nashville, Tennessee, USA.

ISSN 2772-963X https://doi.org/10.1016/j.jacadv.2026.102699

ABBREVIATIONS AND ACRONYMS

AC = aortic closing

AO = aortic opening

AS = aortic stenosis

AVA = aortic valve area

AV AT = aortic valve acceleration time

AV Vmax = aortic jet velocity

BMI = body mass index

ECG = electrocardiography

ET = left ventricular ejection time

ML = machine learning

PCG = phonocardiography

SCG = seismocardiography

TAVR = transcatheter aortic valve replacement

Aortic valve stenosis (AS) is a highly prevalent valvular heart disease and poses a growing public health challenge in the context of an aging population.[1] Although degenerative AS accounts for most cases in developed countries, rheumatic heart disease remains a significant contributor worldwide.[2] The management of AS depends on accurate diagnosis of disease severity.[3] Echocardiography is the primary modality for evaluation and traditionally incorporates 3 main parameters to assess AS severity: effective orifice area by the continuity equation, peak aortic valve (AV) jet velocity (Vmax), and mean AV pressure gradient (MPG).[3,4] The time from AV opening to the peak AV Vmax, conventionally referred to as AV acceleration time (AT), as well as the ratio of AT to left ventricular ejection time (AT/ET), are also associated with AS severity.[5] Traditional echocardiographic indices of AS severity—such as AV Vmax, mean transvalvular gradient, and AV area (AVA)—primarily quantify the magnitude of flow obstruction. In contrast, AT characterizes the temporal pattern of systolic ejection, reflecting delayed time-to-peak outflow in the setting of fixed valvular obstruction. Because AT is closely linked to the timing of mechanical cardiac events during ventricular ejection, it is physiologically coupled to chest-wall vibrations and acoustic signatures measurable with wearable electrocardiography (ECG)-seismocardiography (SCG)-phonocardiography (PCG) sensors. Digital health technologies have emerged as valuable tools in cardiovascular medicine. Traditional ECG remains central to cardiac monitoring, but additional sensing techniques such as SCG and PCG, which capture linear chest wall vibrations and heart sounds, respectively, offer additional physiologic insights.[6,7] These modalities may help detect structural cardiac abnormalities, including coronary artery disease, heart failure, and valvular pathology.[8] Soft bioelectronic sensors now allow noninvasive, real-time monitoring of ECG, SCG, and PCG signals in unimodal or bimodal configurations.[7,9,10]

In this study, the feasibility of a wearable biosensor patch (XCG) that integrates synchronized trimodal ECG, SCG, and PCG signals for the assessment of AS was performed. The primary objective was to quantify the correlation between Doppler-derived AT and sensor-derived AT; the related measure of AT/ET was also assessed. The secondary objective was to apply machine learning (ML) techniques to sensor data to predict AV Vmax.

METHODS

STUDY DESIGN. This feasibility study was a prospective, single-center, observational case-control study conducted at Northwestern University. The study was approved by the Northwestern University Institutional Review Board (IRB #: STU00221912), and all participants provided written informed consent. The investigational device was not used in clinical care.

STUDY POPULATION. Eligibility required age ≥18 years, native trileaflet or bicuspid AVs, and written informed consent. AS severity was classified by American Society of Echocardiography (ASE) guidelines. Severe AS was defined as an AVA ≤1.0 cm^2 together with either an AV Vmax >4.0 m/s or an MPG >40 mm Hg, consistent with transcatheter aortic valve replacement (TAVR) trial criteria[11] Controls were defined as an AV Vmax <2.0 m/s and no more than mild aortic regurgitation. Mild AS was defined as an AVA >1.5 cm^2, an AV Vmax of 2.5 to 2.9 m/s, and an MPG <20 mm Hg; moderate AS was defined as an AV Vmax of 3.0 to 3.9 m/s, AVA 1.0 to 1.5 cm^2, and a mean gradient of 20 to 39 mm Hg. Exclusion criteria included low-flow, low-gradient AS (per ASE guidelines), more than mild aortic regurgitation, prior AV or ascending aortic surgery, atrial fibrillation, contraindication to skin adhesives, pregnancy, inability to acquire analyzable signals, or serious concurrent illness. A total of 65 participants were enrolled in the SENSE-AS (SENsor to Diagnose and Assess SEverity of Aortic Stenosis) study. Ten participants were excluded (6 with low-flow, low-gradient AS; 2 with moderate aortic regurgitation; 1 duplicate enrollment; 1 missing sensor data). The remaining 55 included 15 controls, 11 mild AS, 18 moderate AS, and 11 severe AS subjects. For feasibility and to ensure balanced group sizes in this proof-of-concept study, the first 10 eligible participants from each category were selected for the final analysis, which may limit generalizability of the findings. Controls were matched to the severe AS cohort by age

The authors attest they are in compliance with human studies committees and animal welfare regulations of the authors' institutions and Food and Drug Administration guidelines, including patient consent where appropriate. For more information, visit the Author Center.

Manuscript received January 5, 2026; revised manuscript received February 26, 2026, accepted February 27, 2026.

FIGURE 1 Flow Diagram of Participant Enrollment, Exclusions, and Final Analytic Cohort

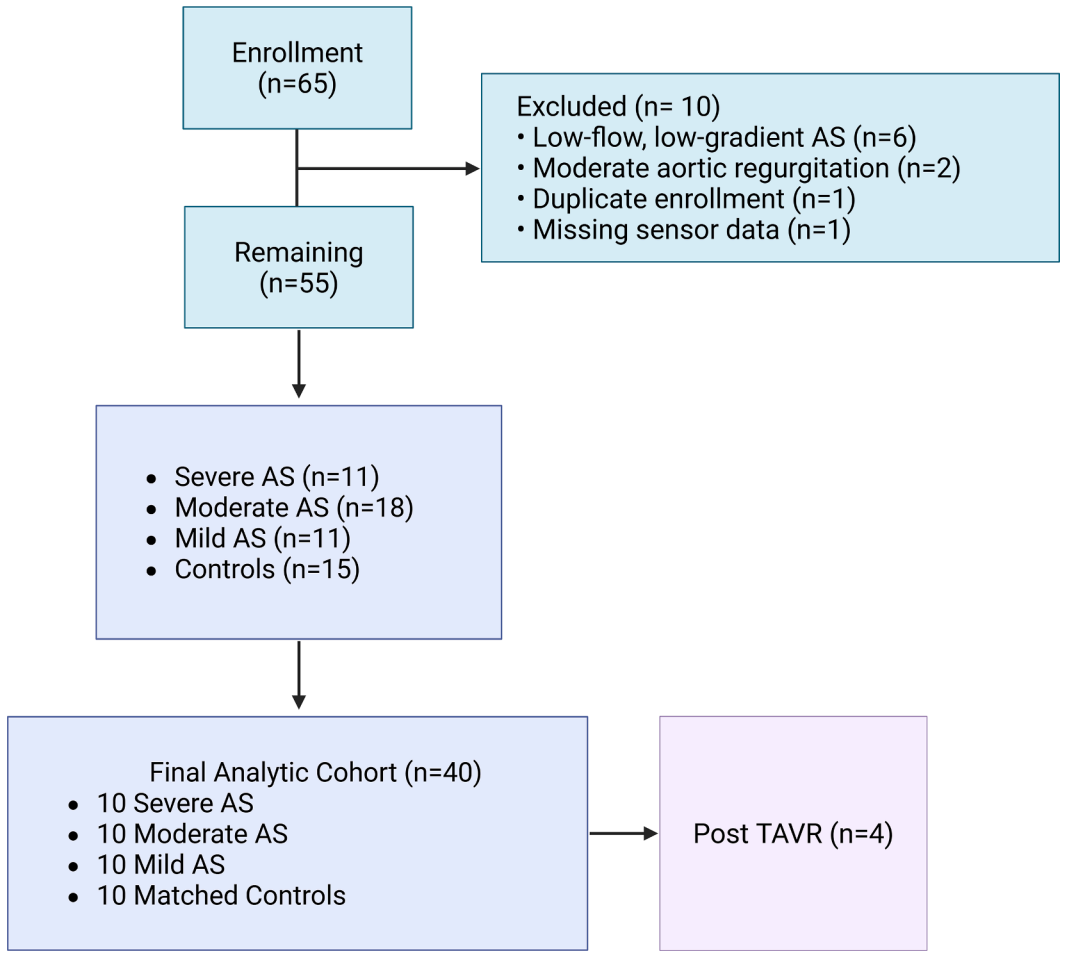

A total of 65 participants were enrolled; 10 were excluded, leaving 55 eligible participants. From these, the first 10 patients meeting inclusion criteria from each group were included in the analysis. The final cohort consisted of 40 participants (10 severe aortic stenosis with 10 matched controls, 10 moderate aortic stenosis, and 10 mild aortic stenosis). Four participants underwent transcatheter aortic valve replacement with post-transcatheter aortic valve replacement repeat sensor measurements. AS = aortic stenosis; TAVR = transcatheter aortic valve replacement.

(±5 years), sex, and body mass index (BMI) (within ± 3 kg/m^2). Baseline cardiovascular comorbidities, including coronary artery disease and prior coronary artery bypass grafting, were documented but were not included as matching variables; therefore, residual confounding by comorbidity burden may persist. The analytic cohort comprised 10 severe, 10 moderate, 10 mild, and 10 control subjects. Four participants subsequently underwent TAVR; repeat postprocedure sensor recordings were collected and analyzed. Study flow is summarized in **Figure 1**.

SENSOR FABRICATION. The XCG sensor consists of components mounted on a flexible printed circuit board (Supplemental Figure 1). A biopotential analog frontend (MAX30001, Analog Instruments) enables high-fidelity ECG capture. Precision, tri-axial accelerometry (LSM6DSO, STMicroelectronics) captures chest wall vibrations and motion. A bone-conductance microphone (V2S200D, Knowles) records acoustic cardiac signatures. An on-board microprocessor (ISP1807, Insight SiP) performs data packaging and transmits signals via Bluetooth to a custom mobile application. The device is encapsulated in soft elastomers. A low-modulus silicone (Silibione 4420) forms the top and bottom layers, cured for 30 minutes at 60 °C. An intermediate silicone (Ecoflex 30) fills the interlayer space and

stabilizes the flexible printed circuit board. The complete assembly is fixtured with spring clamps and cured for 20 minutes at 75 °C.

ECHOCARDIOGRAPHY AND SENSOR PLACEMENT. At the time of clinical transthoracic echocardiography, participants underwent sensor placement immediately following completion of the echocardiographic examination. During clinical transthoracic echocardiography, participants underwent placement of the skin-conformal XCG patch on the left upper chest using hydrogel adhesive after skin preparation. Signals were recorded for 2 4-minute intervals separated by a 1-minute pause. Blood pressure was measured twice at the beginning of the echocardiographic examination, and heart rate was continuously monitored throughout the echocardiographic study and sensor recording period. All participants completed the recording protocol without early termination due to device intolerance, and no device-related adverse events or skin reactions were observed. Data were stored locally and securely transferred for analysis. Echocardiographic parameters (AV Vmax, MPG, AVA, AT, and ET) were measured according to ASE guidelines and served as the gold standard reference.

SENSOR DATA PROCESSING, AT ANALYSIS ALGORITHM, AND MACHINE LEARNING FOR AV VMAX ESTIMATION. Sensor data processing steps are overviewed in Figure 2A. Briefly, data gaps during recording provided fiducial points for precise timestamp alignment between ECG, SCG, and PCG sensor data. Zero-phase filtering then removed noise from ECG (notch, 59-61 Hz), SCG (bandpass, 30-60 Hz), and PCG (bandpass, 20-80 Hz) data (Figure 2B). Polarity-naïve R-peak detection on filtered ECG guided SCG and PCG analysis. Fast Fourier transform analysis identified heart sound regions following each identified R-peak on the ECG. Within the first heart sound, further peak detection isolated the aortic opening (AO) peak in filtered SCG and PCG signals. The second power increase in the heart sound frequency band marked aortic closing (AC). Individual SCG and PCG systolic segments were aligned to the AO point and ensemble averaged (Figure 2C). A signal-quality index threshold—based on the 80th percentile of the Euclidean distance from each segment to the ensemble reference—was applied to exclude noisy or erroneously detected beats. Comparing thresholds between the 50th and 95th percentiles revealed that the 80th percentile threshold maximized data retention while sufficiently denoising input data.

Beat-to-beat ET was derived from AO to AC duration. The processing approach calculated 2 AT estimates from each sensor data, referred to in this work as nonpathologic and pathologic AT. Nonpathologic AT was extracted from the ensemble SCG trace as previously described in healthy patients.[12,13] For murmur analysis, AO and AC timing from segments retained by the signal-quality index filter guided extraction of raw PCG segments. Averaged power spectra from raw PCG signals aligned on AO produced a frequency representation of systolic murmur characteristics. In the average spectrum, enveloping frequency content $>$ 100 Hz identified the shape of the observed murmur. The first peak of the murmur following AO estimated the pathologic AT (Figure 2D). A subsequent algorithm using the ratio of the high frequency (>100 Hz) murmur energy before and after S1 classified each patient as having a pathologic or nonpathologic AT. Sensitivity comparisons between average spectra with increased heartbeat counts determined the minimum recording duration required for stable AT estimation for each patient.

A 2-dimensional convolutional neural network with a regressive output layer was developed to estimate AV Vmax and simultaneously classify AS severity. Preprocessing followed the procedures above, and individual SCG and PCG segments from both recording intervals were used as inputs. The model used 27,435 parameters to represent input data. A custom patient-level data loader ensured balanced AS severity representation in test-train partitions and prevented data leakage by assigning entire patients, not individual heartbeats, exclusively to training (80%) or testing (20%) sets. The testing and training data set did not include post-TAVR data. Because of the small data set, Monte Carlo cross-validation was performed to randomize 20 unique train-test partitions and assess model generalizability and repeatability within the data set. A custom dual-task loss function combined weighted AV Vmax mean absolute error with 4-way cross-entropy classification loss to guide model learning toward both objectives. Each of the 20 model iterations was trained for up to 100 epochs with early stopping after 10 epochs without improvement in AV Vmax error. Model iterations that converged in $>$ 20 epochs were considered sufficiently trained and retained for further analysis. Eighty percent of Monte Carlo cross-validation reached the prespecified convergence threshold. A modified mathematical approach estimated the mean transvalvular pressure gradient from predicted AV Vmax using a second-order polynomial derived from echocardiographic data.[14]

FIGURE 2 Aortic Valve Acceleration Time Algorithm Overview

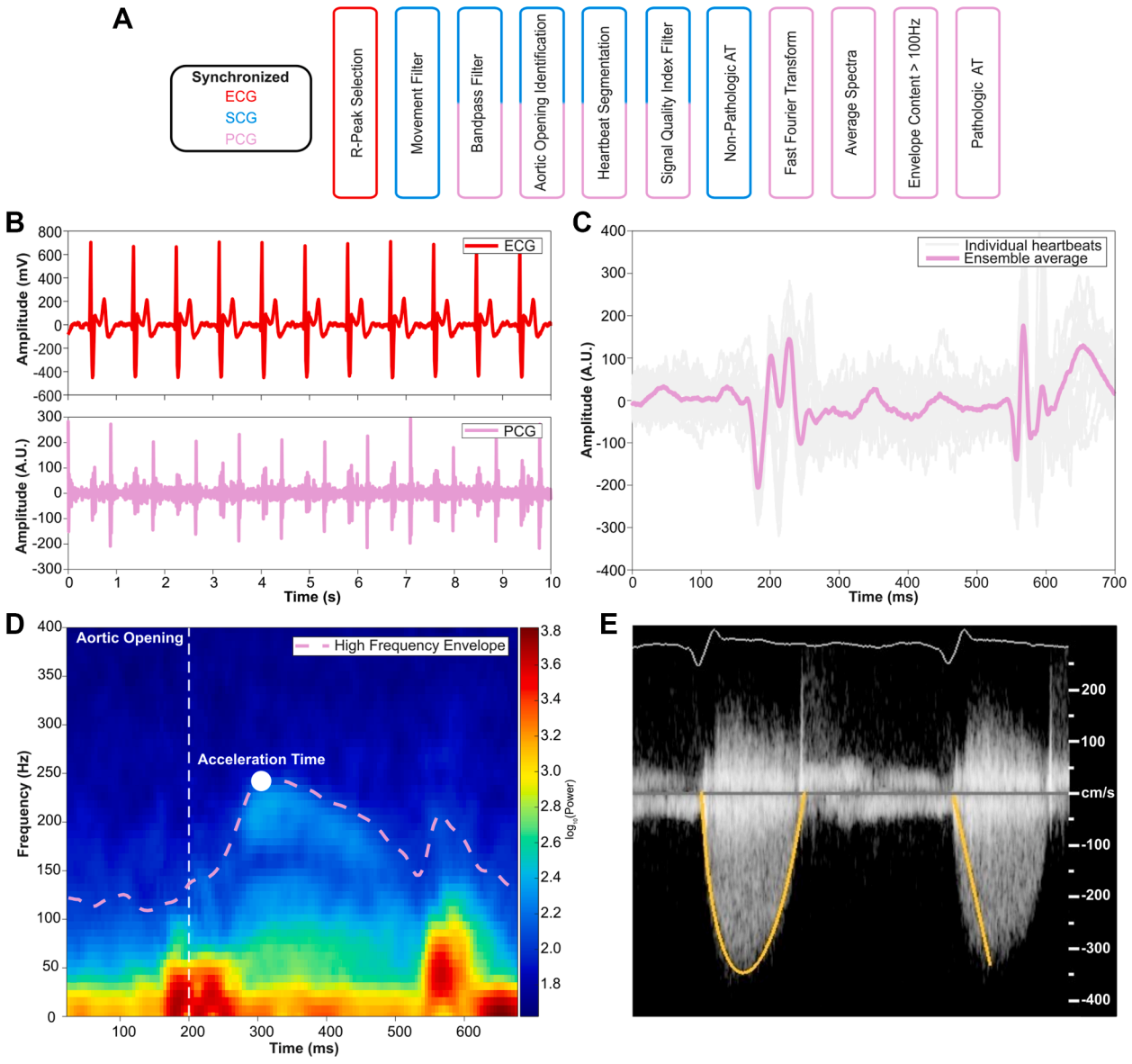

(A) Demonstrates sequence of processing steps necessary to calculate peak acceleration time. Colors represent data stream used in each step. B to E all depict data from the same patient. (B) Depicts representative filtered sensor data. Electrocardiography (top) after 59-61 Hz notch filtering, phonocardiography (bottom) after 20-80 Hz bandpass filtering. (C) Showcases representative phonocardiography heartbeat segmentation prior to averaging spectra. (D) Illustrates a representative average spectrum of phonocardiography data from a patient with aortic stenosis. The envelope is calculated from high frequency murmur content. (E) Provides Doppler echocardiography image recorded immediately prior to sensor recordings in B to D. ECG = electrocardiography; PCG = phonocardiography; SCG = seismocardiography.

DATA COLLECTION AND ANALYSIS. Baseline demographic and clinical characteristics were collected from medical records and verified at consent. The primary endpoint was the correlation between sensor-derived AV AT with Doppler-derived AV AT, and the associated AT/ET ratio. The secondary endpoint was the correlation between sensor-derived AV Vmax predicted from the convolutional neural network model and Doppler AV Vmax. Additional endpoints included device tolerability and reproducibility. Continuous variables were summarized as mean ± SD or median [Quartile 1, Quartile 3], and

TABLE 1 Baseline Clinical and Echocardiographic Characteristics of the Study population

	All Patients (N = 40)	Control (n = 10)	Mild (n = 10)	Moderate (n = 10)	Severe (n = 10)	*P* Value
Clinical data						
Female	22 (55.0)	7 (70.0)	3 (30.0)	5 (50.0)	7 (70)	0.217
Coronary artery disease	19 (47.5)	5 (50.0)	2 (20.0)	7 (70.0)	5 (50.0)	0.164
CABG	3 (7.5)	1 (10.0)	1 (10.0)	1 (10.0)	0 (0.0)	0.782
Bicuspid AV	6 (15.0)	0 (0.0)	6 (60.0)	0 (0.0)	0 (0.0)	<0.001
Age (y)	77.8 (9.5)	78.6 (6.8)	74.6 (11.5)	78.2 (12.0)	79.7 (7.2)	0.67
Heart rate (beats/min)	70.8 (10.5)	73.4 (7.4)	64.2 (10.1)	75.4 (13.3)	70.1 (7.9)	0.082
BMI (kg/m^2)	26.3 (4.7)	23.9 (3.8)	26.8 (4.1)	27.5 (6.1)	26.9 (4.3)	0.336
BSA m^2	1.78 (0.24)	1.68 (0.20)	1.87 (0.22)	1.82 (0.28)	1.75 (0.25)	0.361
Ejection fraction (%)	65 (7)	65 (7)	63 (7)	64 (7)	68 (8)	0.417
Systolic blood pressure (mm Hg)	134 (16)	128 (14)	137 (15)	140 (21)	133 (10)	0.378
Diastolic blood pressure (mm Hg)	70 (10)	68 (13)	69 (10)	73 (6)	69 (11)	0.77
Echocardiographic data						
Acceleration time (ms)	91 (26)	70 (11)	71 (17)	107 (9)	119 (20)	<0.001
Ejection time (ms)	297 (33)	270 (20)	293 (31)	298 (10)	327 (37)	<0.001
Acceleration time/ejection time ratio (AT/ET)	0.31 (0.07)	0.26 (0.04)	0.24 (0.04)	0.36 (0.03)	0.36 (0.04)	<0.001
Max velocity (AVmax) m/s	2.9 (1)	1.6 (0.4)	2.6 (0.2)	3.4 (0.2)	4.1 (0.1)	<0.001
AV mean gradient (mm Hg)	22 (14)	5 (2)	14 (2)	27 (5)	41 (4)	<0.001
LVOT diameter (cm)	2.03 (0.21)	2.02 (0.21)	2.11 (0.14)	2.03 (0.22)	1.96 (0.25)	0.465
AVA (cm^2)	1.5 (0.88)	2.58 (0.98)	1.62 (0.37)	1.05 (0.25)	0.75 (0.22)	<0.001
Indexed SVI	44.6 (11)	45.2 (16.4)	47.0 (8.5)	42.3 (7.6)	43.80 (10.5)	0.81

Values are mean ± SD, median (Quartile 1, Quartile 3), or n (%).
AV = aortic valve; AVA = aortic valve area; BMI = body mass index; BSA = body surface area; LVOT = left ventricular outflow tract; SVI = stroke volume index.

categorical variables as counts (%). Between-group comparisons were conducted with analysis of variance (ANOVA)/Kruskal-Wallis for continuous variables and the chi-square/Fisher exact tests for categorical variables, as appropriate. Analyses were performed in R (version 2024.12.1 + 563). Intraobserver and interobserver variability for echocardiographic AT and ET was assessed across the full cohort by comparing independent measurements from 2 observers (L.H., E.T.). Agreement was evaluated using mean absolute differences and SDs of the differences (Supplemental Table 1). A 2-sided *P* value <0.05 was considered statistically significant. Between-group comparisons of sensor-derived data were performed using one-way ANOVA with post hoc pairwise Tukey tests when indicated by ANOVA results (*scipy.stats*, version 1.16). The area under the receiver operating characteristic curve (AUROC) for classification tasks was computed using the roc_auc_score function from *scikit-learn* (version 1.7.2).

RESULTS

BASELINE CLINICAL AND ECHOCARDIOGRAPHIC CHARACTERISTICS. Forty participants were included in the final analysis: 10 with severe AS, 10 with moderate AS, 10 with mild AS, and 10 controls without significant valve disease who were matched to the severe AS subjects. The mean age was 77.8 years and 55% were female. Baseline clinical and echocardiographic characteristics are presented in **Table 1** and demonstrated expected graded differences across AS severity groups, with higher AV Vmax and MPG, smaller AVA, and longer AV AT with more advanced disease.

SENSOR ACCELERATION TIME AND EJECTION TIME. Sensor AV AT derived from deterministic processing of sensor data revealed strong agreement with Doppler-derived AV AT (r = 0.85; 95% CI: 0.73-0.92; *P* < 0.001) (**Figure 3D**). When stratified by AS severity, pairwise AT comparisons indicated clear separation of controls and mild AS patients from moderate and severe AS patients for both sensor- and echocardiography-derived AT (all *P* < 0.01) (**Figures 3A and 3B**). Bland-Altman analysis quantified the limits of agreement between sensor-derived AT and echocardiography, with a bias of −5.3 ms and limits of agreement from −35.1 ms to 24.6 ms (**Figure 3C**). Sensor-derived AT/ET ratio differentiated AS severity similar to AT, separating control and mild from moderate and severe AS groups (all *P* < 0.001) (Supplemental Figure 2A). Sensor AT/ET ratio

FIGURE 3 Acceleration Time Algorithm Results

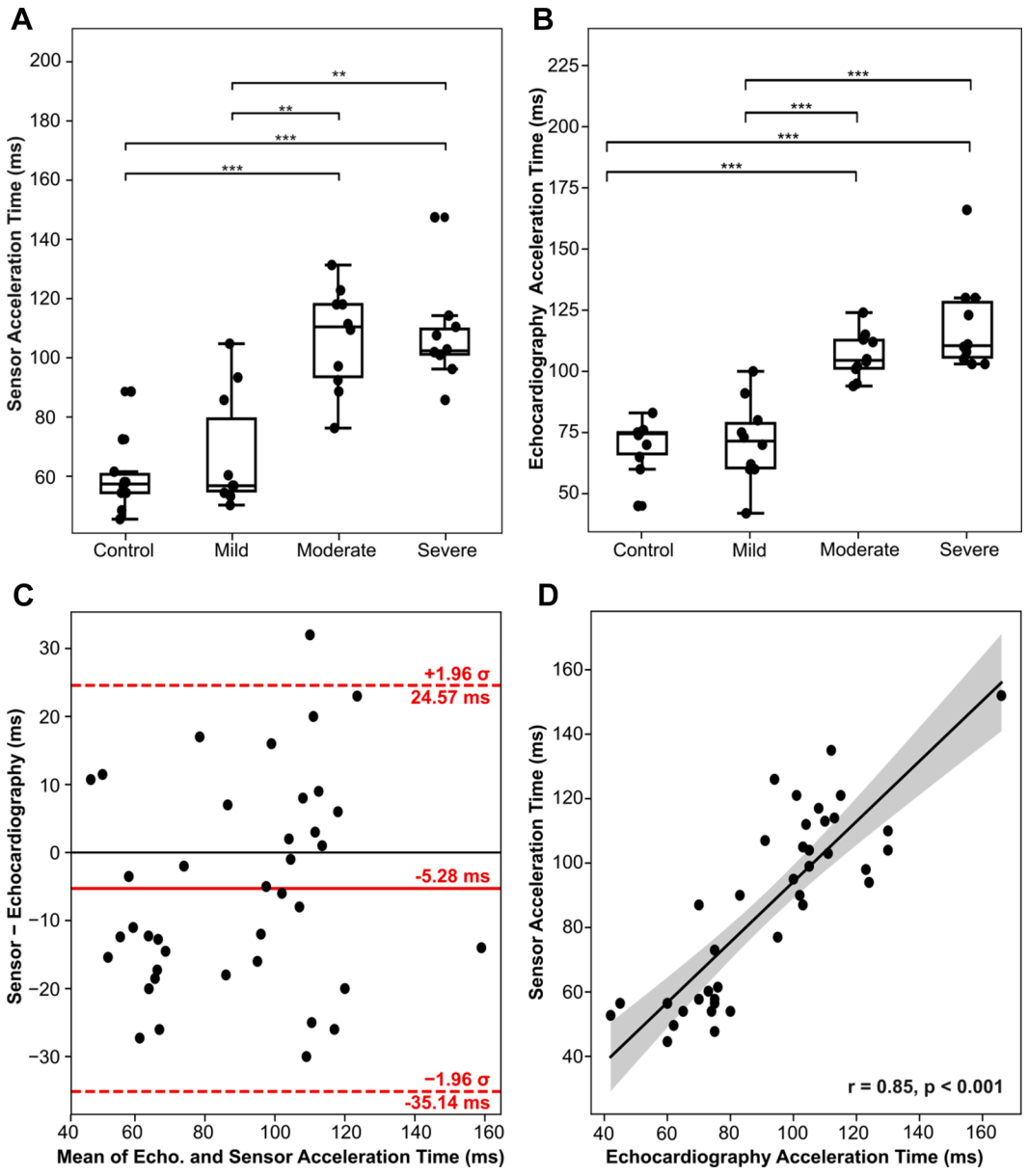

(A) Compares sensor aortic valve acceleration time and aortic stenosis severity classification. (B) Compares echocardiography acceleration time and aortic stenosis severity classification. $^{**}P < 0.01$, $^{***}P < 0.001$. (C) Presents Bland-Altman analysis of sensor predicted acceleration time compared to echocardiography. Solid red line depicts bias, and dashed red line depicts 95% CI of sensor bias. (D) Demonstrates correlation between sensor calculated peak acceleration time and echocardiography-derived peak acceleration time. Shaded gray region represents 95% CI.

correlated well with echocardiographic AT/ET (r = 0.77, $P < 0.001$) (Supplemental Figure 2B). Comparison across average spectra from different data durations revealed that 25 heartbeats were sufficient to achieve a stable murmur spectrogram ($P < 0.05$, Supplemental Figure 3). Repeatability was high: sensor AT estimated from the first recording correlated strongly with sensor AT estimated from the second recording (r = 0.87, $P < 0.001$) (Supplemental Figure 4). Intraobserver

FIGURE 4 Machine Learning Results on Testing Data

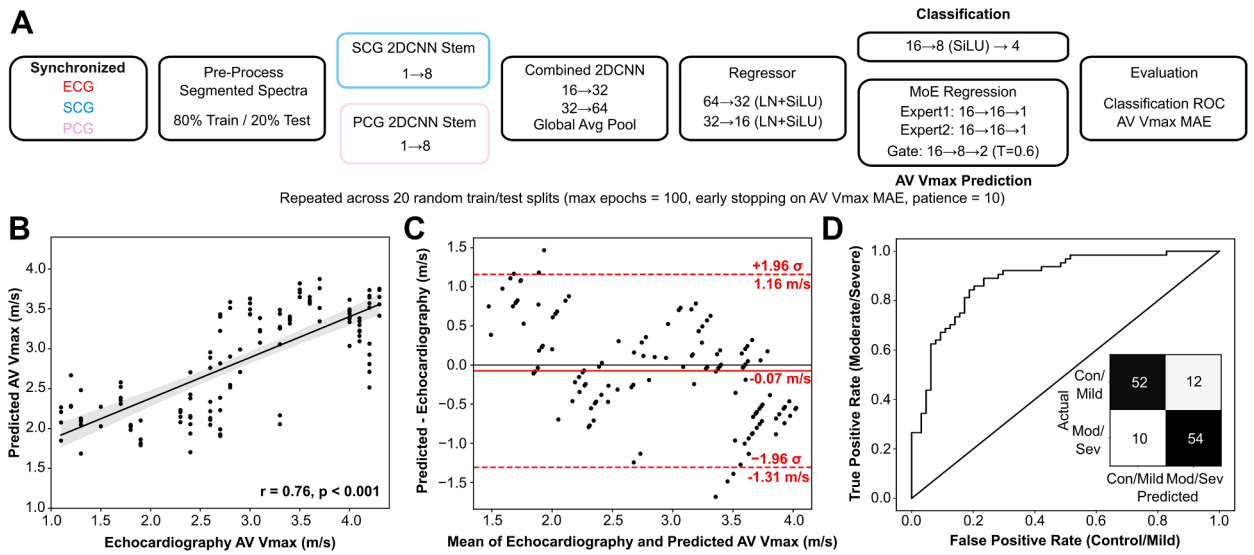

(A) Illustrates the architecture and evaluation strategy of the machine learning model. Colors represent data stream used in each step. (B) Depicts correlation between sensor predicted aortic valve Vmax and echocardiographic aortic valve Vmax measurements. Shaded gray region represents 95% CI of agreement. (C) Showcases Bland-Altman analysis of sensor and echocardiographic data. Red line indicates bias, red dashed line indicates 95% CI. (D) Demonstrates receiver-operator curve for binary classification task between control/mild and moderate/severe with an inlaid classification task confusion matrix (AUROC of 0.888). 2DCNN = 2D convolutional neural network; AUROC = area under the receiver operating characteristic curve; AV = aortic valve; LN = layer normalization; MAE = mean absolute error; ROC = receiver operating characteristic; SILU = sigmoid linear unit; other abbreviations as in Figure 2.

and interobserver variability for Doppler AT was 6.6 ± 5.1 ms and 3.7 ± 4.0 ms, respectively (Supplemental Table 1).

DEEP LEARNING MODELING OF AORTIC STENOSIS PARAMETERS. Sensor AV Vmax predicted by ML models on unseen patient data demonstrated good agreement with echocardiographic AV Vmax (r = 0.76; 95% CI: 0.68-0.83; $P < 0.001$) (Figure 4A and 4B). Bland-Altman limits of agreement for AV Vmax ranged from −1.31 m/s to 1.16 m/s (Figure 4C). Classification accuracy, defined in the study as discrimination of control and mild patients from moderate and severe, achieved an AUROC of 0.888 and F-score of 0.831 (Figure 4D). For MPG estimation, a second-order polynomial fit between echocardiographic AV Vmax and MPG data achieved $R^2 = 0.947$. When applied to sensor AV Vmax predictions, fit polynomial-derived MPG predictions produced a similar performance (r = 0.75, $P < 0.001$).

POST-TRANSCATHETER AORTIC VALVE REPLACEMENT COMPARISONS. In the cohort, 4 patients underwent TAVR during follow-up. Preprocedural and postprocedural sensor recordings revealed distinct differences in systolic frequency content (Figures 5C and 5D). In this small patient data set, further data processing demonstrated reductions in peak AT following TAVR, observed in both sensor and echocardiographic measurements ($P < 0.01$ for all) (Figure 5E). The ML model predictions on post-TAVR sensor data held out from model training and testing reflected reductions in predicted AV Vmax, in line with echocardiographic measurements ($P < 0.01$ for all) (Figure 5F).

DISCUSSION

In this feasibility study, we evaluated a wearable, multimodal cardiac sensor for the noninvasive assessment of AS. Several notable findings should be highlighted. First, both sensor-derived AT and the AT/ET ratio demonstrated strong associations with AS severity based on echocardiographic guidelines. Second, sensor-derived AT showed high correlation and minimal bias compared with Doppler AT, despite relying solely on deterministic signal processing without ML assistance. Third, sensor-derived estimates of AV Vmax correlated well with Doppler AV Vmax, also with limited bias (Central Illustration). Finally, among a small number of patients who later underwent TAVR, sensor recordings captured the expected postprocedural physiologic improvements,

FIGURE 5 Pre- and Post-Transcatheter Aortic Valve Replacement

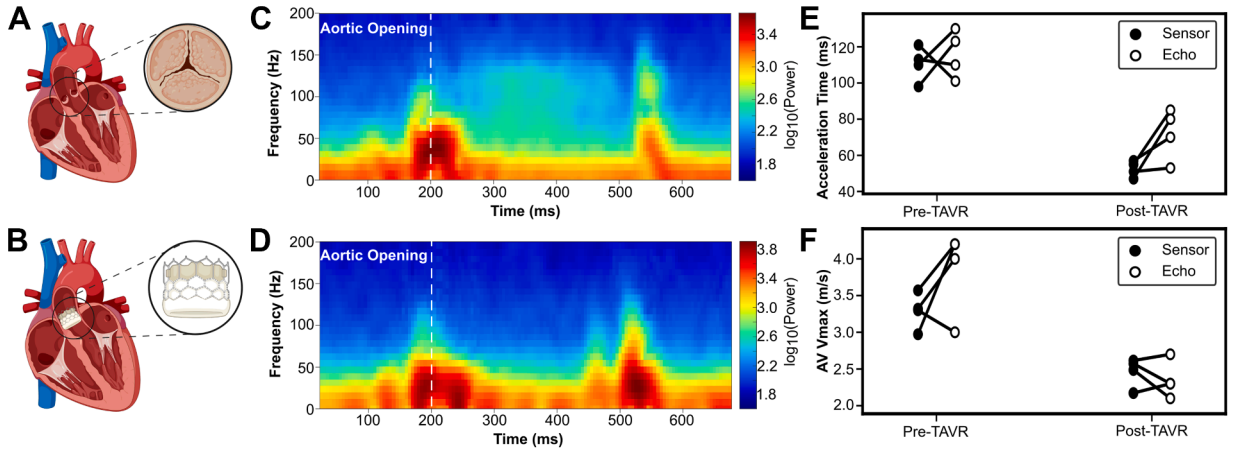

(A) Depicts schematic of diseased aortic valve, (B) and after transcatheter aortic valve replacement (Created in BioRender, Rogers J, 2026, https://BioRender.com/v40pur1). C and D both use data from the same patient. (C) Illustrates the average spectrum of patient sensor data prior to valve replacement, and (D) Illustrates the average spectrum following valve replacement. (E) Compares sensor (filled) and echocardiography (empty) aortic valve acceleration time values before and after transcatheter aortic valve replacement. (F) Compares sensor (filled) and echocardiography (empty) aortic valve Vmax before and after transcatheter aortic valve replacement. In E and F, black lines connect each patient's sensor and echocardiography measurement Abbreviation as in **Figure 1**.

including reductions in murmur intensity (**Figures 5C and 5D**), AT and AV Vmax.

Current clinical guidelines emphasize the importance of timely surveillance in AS, as the only definitive treatment is surgical or transcatheter valve replacement, and no medical therapy has been shown to slow or reverse disease progression.[15] Although echocardiography remains the diagnostic gold standard, it requires specialized equipment and expertise and is not always readily accessible. Even though continuous monitoring is neither practical nor necessary for slowly progressive diseases such as AS, this biosensor technology may facilitate accessible and intermittent monitoring for diagnosis and surveillance, especially in settings with limited access to echocardiography.

AT reflects the rate of systolic flow acceleration across the AV and serves as a sensitive marker of valvular obstruction severity.[16,17] It has long been recognized as a physiologic indicator of AS severity, reflecting delayed systolic ejection and increased valvular obstruction.[18-20] The ratio of acceleration to ejection time (AT/ET) further integrates the hemodynamic load imposed by the valve by providing an adjustment for heart rate.[20] In contemporary studies, an AT/ET ≥0.32 has been associated with higher cardiovascular mortality and heart-failure hospitalization, while a cutoff of 0.35 accurately identified symptomatic or severe AS.[21,22]

The algorithms presented here advance previous efforts to increase the scalability of AS diagnosis through explainable estimation of clinically and physiologically relevant AS parameters. Several prior studies applied "black box" artificial intelligence to individual modalities such as ECG,[23-26] SCG,[27] PCG,[28] or echocardiography images[29-32] to stratify AS severity without producing clinically meaningful AS parameters. Shokouhmand et al leveraged interpretable ML using SCG and gyrocardiogram-derived features to stratify AS. However, calculated features had unclear relationships with AS relevant physiology and required human annotation[33] In contrast, our automated signal processing approach presented here calculates AT and ET, known to discriminate high- and low-risk AS.[16,17] We offer a repeatable, automated, and explainable alternative to prior efforts.

Our ML approach demonstrates the first patient demographic naïve wearable-based AV Vmax and MPG estimation capabilities evaluated on data from the full AS pathology range. Ebrahimkhani et al previously explored prediction of AV Vmax using unimodal wearable SCG signals and demographic data,[27] whereas our approach achieved strong performance without demographic inputs, benefiting from PCG-derived murmur content. Our model additionally uses a sufficiently low number of parameters to enable on-sensor function. Other efforts

CENTRAL ILLUSTRATION **Estimation of Aortic Valve Functional Parameters and Severity Stratification Using a Wearable Sensor in Patients With Aortic Stenosis**

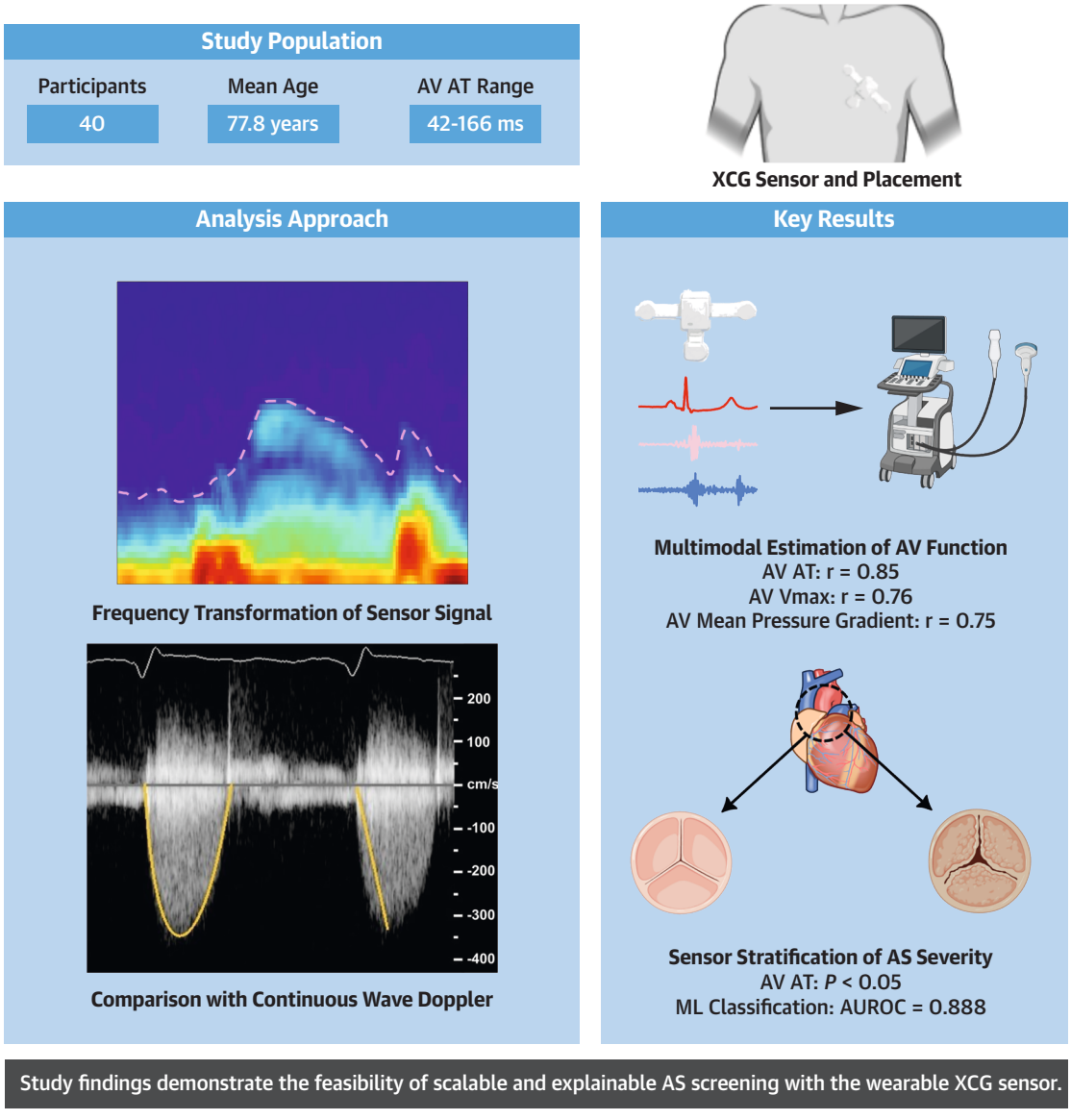

The top row describes the study population and diagrams sensor placement. The lower left panel provides a high-level overview of processed sensor signal output, murmur signal enveloping, and comparison to clinical continuous wave Doppler. The lower **right** panel summarizes study results including correlation with clinical echocardiography metrics (all $P < 0.001$) and severity stratification. AT = acceleration time; ML = machine learning; Vmax = peak velocity; other abbreviation as in Figure 5.

used traditional stethoscope PCG and regressed single spectral parameters to AV Vmax or MPG.[34-36] Sensor AT estimates correlated reasonably well with echocardiographic AV Vmax (r = 0.72) (Supplemental Figure 5). Regressing sensor AT to AV Vmax offers a more explainable but slightly less accurate alternative to the ML estimation in this work.

The similar accuracy for MPG and AV Vmax prediction (r = 0.75, 0.76, respectively) compared to echocardiography underscores the clinical relevance

of noninvasive estimation of AV functional decline in this work. Expanding the training data set beyond the limited population included in this study—particularly at the severity extremes—may further enhance model precision and classification performance.

Importantly, post-TAVR data were not included in model training or testing. Although the model detected reductions in AV Vmax in unseen post-TAVR patient recordings, these findings are based on a limited number of patients and should be interpreted as exploratory and hypothesis-generating. As such, no conclusions regarding post-intervention performance or clinical utility of the platform for TAVR monitoring can be drawn from this subgroup. Even though an implantable trimodal ECG-SCG-PCG device has been developed by others,[37] the XCG sensor is, to our knowledge, the first wearable platform enabling synchronized ECG, SCG, and PCG capture. The multimodal design leverages the complementary frequency response profiles of accelerometers and contact microphones: SCG performs optimally at <50 Hz for capturing S1 and S2, whereas PCG has superior sensitivity to higher-frequency murmur components (>50-100 Hz). Our analysis methods rely on the synchronized trimodal cardiac information captured by the XCG sensor. Specifically, ECG facilitated reliable heartbeat segmentation; SCG detected 15% more AO/AC pairs than PCG for ET and nonpathologic AT calculation; and PCG provided richer murmur content with superior sensitivity than SCG (Supplemental Figure 6), critical for pathologic AT calculation and murmur analysis. These modalities, integrated in the soft, skin-conformal XCG sensor, support continuous, noninvasive monitoring of AV function and echocardiographic parameters in real time with our analysis approaches.

In the context of AS, such a wearable platform supports ease of use and potential patient self-application to aid in the diagnosis of AS in broader settings, such as at home or at community health events. In particular, precise auscultatory localization is not required; high-quality S1, S2, and systolic murmur signals can be obtained across a relatively broad parasternal and mid-precordial region (eg, along the left sternal border spanning approximately the 2nd-4th intercostal spaces). Minor spatial variation within this region does not result in abrupt degradation of acoustic or mechanical signal quality. With minimal instruction using simple anatomical anchor points (sternal border and intercostal space landmarks), patients could feasibly obtain periodic short recordings at home or in community settings. The multimodal integration of ECG, SCG, and PCG further enhances robustness to modest placement variability by preserving electrical-mechanical timing features. However, further work to determine the influence of motion artifacts and other sources of noise on sensor performance in other environments is necessary to evaluate the feasibility of sensor use outside of controlled clinical settings. In addition to AS, such XCG devices could enable screening for other valvular lesions and telehealth monitoring of conditions including patients with dynamic left ventricular outflow tract obstruction.

STUDY LIMITATIONS. Several limitations warrant consideration. First, the clinical echocardiography workflow prevented simultaneous sensor placement during patient imaging and comparison between identical cardiac beats. However, the sensor was placed immediately after completion of the echocardiogram, and no changes in the hemodynamic status of the patient would be expected. Second, the sensor recorded from each patient for a relatively short amount of time. Analysis methods provided stable estimates of AV AT and Vmax well within this time frame and demonstrated the feasibility of short recording for mass screening. However, the recording duration limits insights into long-term wearability and performance of the XCG sensor, particularly during exercise. Third, although reproducibility was generally strong, 6 participants demonstrated $>$ 20 ms differences in AT between recordings. Signal review suggested contributions from motion artifacts, local noise, or subtle changes in signal envelope morphology, which could be more pronounced during ambulatory or home-based use. Fourth, we excluded patients with moderate or greater aortic regurgitation and patients with low-flow, low-gradient AS. Future investigations will evaluate these patient populations, which will be important for real-world application. Fifth, we employed a strict definition of severe AS consistent with clinical trial definitions.[11] Patients may have symptomatic AS and not fulfill these criteria. Although baseline comorbidity prevalence did not differ significantly across groups, this study was not designed or powered to evaluate the independent effects of common cardiovascular and noncardiac comorbidities on signal quality or model performance, which may limit generalizability to more heterogeneous populations. Sixth, higher BMI may result in degraded SCG and PCG signal quality, although this was not observed in our cohort of patients with predominantly normal BMIs, and further studies could investigate generalizability to higher BMI patients. Finally, the ML analyses were conducted in a relatively small, single-center data set and lack external validation. Although participant-

level separation was used to mitigate data leakage, the resulting models should be considered exploratory and hypothesis-generating. Validation in larger, independent, multicenter cohorts is required to determine generalizability and clinical utility.

CONCLUSIONS

This case-control study demonstrates the feasibility of using a wearable multimodal cardiac sensor to detect and stratify AS severity. These findings support the feasibility and technical viability of a wearable multimodal sensing approach for scalable physiologic assessment of AS severity, forming a foundation for future prospective validation studies. Our results also support the possibility of using the XCG for other valvular lesions, longitudinal monitoring, and assessment of impact of AS on patients' lives before and after AV replacement.

FUNDING SUPPORT AND AUTHOR DISCLOSURES

This work was funded by the Querrey Simpson Institute for Bioelectronics. Dr Rogers is a co-founder of Sibel Health, Inc. Dr Cremer has relationships with GE Healthcare, Boston Scientific, Cleerly Health, Kiniksa Pharmaceuticals, CardiolRx Therapeutics, Ventyx Biosciences, and Monte Rosa Therapeutics. All other authors have reported that they have no relationships relevant to the contents of this paper to disclose.

ADDRESS FOR CORRESPONDENCE: Dr Paul C. Cremer, Northwestern University, Feinberg School of Medicine, Bluhm Cardiovascular Institute, 676 N St Clair St: Suite 700, Chicago, Illinois 60611, USA. E-mail: paul.cremer@nm.org. OR Dr Yayun Du, Vanderbilt University, Electrical and Computer Engineering, Nashville, Tennessee 37240, USA. E-mail: yayun.du@vanderbilt.edu.

PERSPECTIVES

COMPETENCY IN MEDICAL KNOWLEDGE: AV AT and the AT/ET ratio reflect AS severity. A chest-worn multimodal wearable sensor can reliably measure AT and AT/ET, showing strong agreement with Doppler echocardiography and consistent differentiation across AS severity groups. This multimodal sensor appears feasible for low-cost and accessible detection of AS.

TRANSLATIONAL OUTLOOK: Larger, multicenter studies with diverse populations and longer monitoring durations are needed to validate wearable-based AS assessment, including performance during daily activity and exercise. Future research should also evaluate the device in broader AS phenotypes, such as low-flow, low-gradient AS and mixed valvular disease.

REFERENCES

1. Bonow RO, Greenland P. Population-wide trends in aortic stenosis incidence and outcomes. *Circulation*. 2015;131(11):969-971. https://doi.org/10.1161/CIRCULATIONAHA.115.014846

2. Peeters FECM, Meex SJR, Dweck MR, et al. Calcific aortic valve stenosis: hard disease in the heart. *Eur Heart J*. 2018;39(28):2618-2624. https://doi.org/10.1093/eurheartj/ehx653

3. Otto CM, Nishimura RA, Bonow RO, et al. 2020 ACC/AHA guideline for the management of patients with Valvular Heart Disease: a report of the American College of Cardiology/American Heart Association Joint Committee on Clinical Practice Guidelines. *J Am Coll Cardiol*. 2021;77(4):e25-e197. https://doi.org/10.1016/j.jacc.2020.11.018

4. Vahanian A, Beyersdorf F, Praz F, et al. 2021 ESC/EACTS guidelines for the management of valvular heart disease: developed by the Task Force for the management of valvular heart disease of the European Society of Cardiology (ESC) and the European Association for Cardio-Thoracic Surgery (EACTS). *Eur Heart J*. 2022;43(7):561-632. https://doi.org/10.1093/eurheartj/ehab395

5. Gamaza-Chulián S, Díaz-Retamino E, Camacho-Freire S, Ruiz-Fernández D, Gutiérrez-Barrios A, Oneto-Otero J. Acceleration time and ratio of acceleration time to ejection time in aortic stenosis: new echocardiographic diagnostic parameters. *J Am Soc Echocardiogr*. 2017;30(10):947-955. https://doi.org/10.1016/j.echo.2017.06.001

6. Bhattacharya S, Nikbakht M, Alden A, et al. A chest-conformable, wireless electromechanical e-tattoo for measuring multiple cardiac time intervals. *Adv Electron Mater*. 2023;9(9):2201284. https://doi.org/10.1002/aelm.202201284

7. Chen S, Ouyang Q, Meng X, et al. Starfish-inspired wearable bioelectronic systems for physiological signal monitoring during motion and real-time heart disease diagnosis. *Sci Adv*. 2025;11(14):eadv2406. https://doi.org/10.1126/sciadv.adv2406

8. Ha T, Tran J, Liu S, et al. A chest-laminated ultrathin and stretchable e-tattoo for the measurement of electrocardiogram, seismocardiogram, and cardiac time intervals. *Adv Sci*. 2019;6(14):1900290. https://doi.org/10.1002/advs.201900290

9. Ershad F, Thukral A, Yue J, et al. Ultra-conformal drawn-on-skin electronics for multifunctional motion artifact-free sensing and point-of-care treatment. *Nat Commun*. 2020;11:3823. https://doi.org/10.1038/s41467-020-17619-1

10. Liu Y, Norton JJ, Qazi R, et al. Epidermal mechano-acoustic sensing electronics for cardiovascular diagnostics and human-machine interfaces. *Sci Adv*. 2016;2(11):e1601185. https://doi.org/10.1126/sciadv.1601185

11. Généreux P, Schwartz A, Oldemeyer JB, et al. Transcatheter aortic-valve replacement for asymptomatic severe aortic stenosis. *N Engl J Med*. 2025;392(3):217-227. https://doi.org/10.1056/NEJMoa2405880

12. Piemme TE, Barnett GO, Dexter L. Relationship of heart sounds to acceleration of blood flow. *Circ Res*. 1966;18(3):303-315. https://doi.org/10.1161/01.RES.18.3.303

13. Sørensen K, Schmidt SE, Jensen AS, Søgaard P, Struijk JJ. Definition of fiducial points in the normal seismocardiogram. *Sci Rep*. 2018;8(1):15455. https://doi.org/10.1038/s41598-018-33675-6

14. Zhang Y, Nitter-Hauge S. Determination of the mean pressure gradient in aortic stenosis by Doppler echocardiography. *Eur Heart J*. 1985;6(12):999-1005. https://doi.org/10.1093/oxfordjournals.eurheartj.a061821

15. Roberts WC, Ko JM. Frequency by decades of unicuspid, bicuspid, and tricuspid aortic valves in adults having isolated aortic valve replacement for aortic stenosis, with or without associated aortic regurgitation. *Circulation*. 2005;111(7):920-925. https://doi.org/10.1161/01.CIR.0000155623.48408.C5

16. Maréchaux S, Tribouilloy C. Acceleration time in aortic stenosis. *Circ Cardiovasc Imaging*. 2021;14(1):e012234. https://doi.org/10.1161/CIRCIMAGING.120.012234

17. Ben Zekry S, Saad RM, Ozkan M, et al. Flow acceleration time and ratio of acceleration time to ejection time for prosthetic aortic valve function. *JACC Cardiovasc Imaging*. 2011;4(11):1161-1170. https://doi.org/10.1016/j.jcmg.2011.08.012

18. Barnes RW, Rittenhouse EA, Miller EV. Doppler ultrasonic assessment of aortic stenosis by analysis of axillary arterial blood velocity upstroke time. *Chest*. 1976;70(1):48-50. https://doi.org/10.1378/chest.70.1.48

19. Hatle L, Angelsen BA, Tromsdal A. Non-invasive assessment of aortic stenosis by Doppler ultrasound. *Br Heart J*. 1980;43(3):284-292. https://doi.org/10.1136/hrt.43.3.284

20. Parisi AF, Salzman SH, Schechter E. Systolic time intervals in severe aortic valve disease: changes with surgery and hemodynamic correlations. *Circulation*. 1971;44(4):539-547. https://doi.org/10.1161/01.CIR.44.4.539

21. Altes A, Thellier N, Bohbot Y, et al. Relationship between the ratio of acceleration time/ejection time and mortality in patients with high-gradient severe aortic stenosis. *J Am Heart Assoc*. 2021;10(23):e021873. https://doi.org/10.1161/JAHA.121.021873

22. Einarsen E, Cramariuc D, Bahlmann E, Midtbø H, Chambers JB, Gerdts E. Higher acceleration/ejection time ratio predicts impaired outcome in aortic valve stenosis. *Circ Cardiovasc Imaging*. 2021;14(1):e011467. https://doi.org/10.1161/CIRCIMAGING.120.011467

23. Hata E, Seo C, Nakayama M, Iwasaki K, Ohkawauchi T, Ohya J. Classification of aortic stenosis using ECG by deep learning and its analysis using Grad-CAM. In: *Proceedings of the 42nd annual international conference of the IEEE Engineering in Medicine and Biology Society (EMBC)*. IEEE; 2020:1548-1551. https://doi.org/10.1109/EMBC44109.2020.9175151

24. Kwon J, Lee SY, Jeon K, et al. Deep learning-based algorithm for detecting aortic stenosis using electrocardiography. *J Am Heart Assoc*. 2020;9(7):e014717. https://doi.org/10.1161/JAHA.119.014717

25. Cohen-Shelly M, Attia ZI, Friedman PA, et al. Electrocardiogram screening for aortic valve stenosis using artificial intelligence. *Eur Heart J*. 2021;42(30):2885-2896. https://doi.org/10.1093/eurheartj/ehab153

26. Aminorroaya A, Dhingra LS, Sangha V, et al. Deep learning-enabled detection of aortic stenosis from noisy single lead electrocardiograms. Preprint. *medRxiv*. Posted October 2, 2023. https://doi.org/10.1101/2023.09.29.23296017

27. Ebrahimkhani M, Johnson EMI, Sodhi A, et al. A deep learning approach to using wearable seismocardiography (SCG) for diagnosing aortic valve stenosis and predicting aortic hemodynamics obtained by 4D flow MRI. *Ann Biomed Eng*. 2023;51(12):2802-2811. https://doi.org/10.1007/s10439-023-03342-7

28. Ghanayim T, Lupu L, Naveh S, et al. Artificial intelligence-based stethoscope for the diagnosis of aortic stenosis. *Am J Med*. 2022;135(9):1124-1133. https://doi.org/10.1016/j.amjmed.2022.04.032

29. Park J, Kim J, Jeon J, et al. Deep learning-based detection and severity assessment of bicuspid aortic valve stenosis. *J Am Soc Echocardiogr*. 2025;38(8):723-725. https://doi.org/10.1016/j.echo.2025.04.002

30. Krishna H, Desai K, Slostad B, et al. Fully automated artificial intelligence assessment of aortic stenosis by echocardiography. *J Am Soc Echocardiogr*. 2023;36(7):769-777. https://doi.org/10.1016/j.echo.2023.03.008

31. Holste G, Oikonomou EK, Mortazavi BJ, et al. Severe aortic stenosis detection by deep learning applied to echocardiography. *Eur Heart J*. 2023;44(43):4592-4604. https://doi.org/10.1093/eurheartj/ehad456

32. Anul Haq M, Mahendran RK, Khan A, Ali F, Gyani J. Tri-STANet: an advanced framework integrating dual axis transformer and morphological encoding for enhanced AS detection. *Expert Syst Appl*. 2026;297:129372. https://doi.org/10.1016/j.eswa.2025.129372

33. Shokouhmand A, Aranoff ND, Driggin E, Green P, Tavassolian N. Efficient detection of aortic stenosis using morphological characteristics of cardiomechanical signals and heart rate variability parameters. *Sci Rep*. 2021;11(1):23817. https://doi.org/10.1038/s41598-021-03441-2

34. Sun Z, Poh KK, Ling LH, Hong GS, Chew CH. Acoustic diagnosis of aortic stenosis. *J Heart Valve Dis*. 2005;14(2):166-172.

35. Johnson GR, Myers GS, Lees RS. Evaluation of aortic stenosis by spectral analysis of the murmur. *J Am Coll Cardiol*. 1985;6(1):55-63. https://doi.org/10.1016/S0735-1097(85)80253-9

36. Kim D, Tavel ME. Assessment of severity of aortic stenosis through time-frequency analysis of murmur. *Chest*. 2003;124(5):1638-1644. https://doi.org/10.1378/chest.124.5.1638

37. Future Cardia. Future Cardia. Accessed December 10, 2025. https://www.futurecardia.com

KEY WORDS aortic stenosis, telehealth, translational, wearable sensors

APPENDIX For supplemental tables and figures, please see the online version of this paper.